

# Hydrogen blister formation and cracking behavior for various tungsten materials

Y. Ueda <sup>a,\*</sup>, T. Funabiki <sup>a</sup>, T. Shimada <sup>a</sup>, K. Fukumoto <sup>b</sup>,  
H. Kurishita <sup>b</sup>, M. Nishikawa <sup>a</sup>

<sup>a</sup> Graduate School of Engineering, Department of Electronic, Information Systems, Osaka University,  
2-1 Yamada-Oka, Suita, Osaka 565-0871, Japan

<sup>b</sup> Tohoku University, Oarai, Ibaraki 311-1313, Japan

## Abstract

In order to study hydrogen blistering and subsequent cracking behavior of pure W, K-doped W, and La<sub>2</sub>O<sub>3</sub>-doped W, 1 keV H<sub>3</sub><sup>+</sup> (main ion components) ion beams were irradiated at 653 K to fluences up to  $1 \times 10^{25}$  H/m<sup>2</sup>. Two pre-irradiation heat treatments were done for stress relief (900 °C) and recrystallization (1300 °C for pure W and 1500 °C for K-doped and La<sub>2</sub>O<sub>3</sub>-doped W). It was found that blister characteristics and cracking behavior strongly depended on microstructures and dopant materials. For W materials with layered microstructure, blister shapes were mostly spherical-like, while for W materials with recrystallized (or disordered) microstructures, blisters had complicated plateau-like shapes with many cracks. Addition of K or La<sub>2</sub>O<sub>3</sub> dopants increased the number of blisters and exfoliations for both stress relieved and recrystallized W.

© 2004 Elsevier B.V. All rights reserved.

PACS: 52.40.Fd; 61.80.Jh

Keywords: Bubbles and blisters; Ion surface interaction; Tungsten

## 1. Introduction

In DEMO and future commercial reactors, sputtering erosion of plasma facing materials (PFMs) is a serious concern for not only low *Z* materials (beryllium and carbon) but also low activation materials (ferritic steel, vanadium alloy, and SiC) [1]. Therefore, in order to protect plasma facing surface from erosion, tungsten is a leading candidate of PFMs (armor materials). However blistering [2–4] and embrittlement can take place with

hydrogen and helium ion irradiation as well as neutron irradiation. Cracking and exfoliation can take place on these tungsten materials, which enhances erosion and brings about serious effects to core plasmas. Therefore, it is very important to evaluate hydrogen blister formation and subsequent cracking and exfoliation behavior for various tungsten materials under hydrogen plasma exposure. However, comprehensive and reliable databases as well as sufficient understandings on basic processes have not been established.

We have been making hydrogen beam irradiation experiments on tungsten with a steady-state high flux ion irradiation device (HiFIT) for the above-mentioned purpose. It was found that hydrogen blistering and

\* Corresponding author. Tel.: +81 6 879 7236; fax: +81 6 879 7867.

E-mail address: [yueda@eie.eng.osaka-u.ac.jp](mailto:yueda@eie.eng.osaka-u.ac.jp) (Y. Ueda).

subsequent cracking behavior of tungsten was enhanced by carbon addition (>0.3%) to hydrogen ion beam (mainly 1 keV  $H_3^+$ ). The possible mechanism of the enhancement is that tungsten and carbon mixed layer formed on the tungsten surface prevents the implanted hydrogen atoms from leaving the tungsten surface due to low diffusivity of hydrogen in WC layer and low recombination rates of hydrogen atoms on the layer [5–7].

In the present study, characteristics of hydrogen blistering, subsequent cracking formation and exfoliation for various tungsten materials are observed to make a useful database for the selection of tungsten materials for PFMs. Tungsten materials used for the study were pure W, K-doped tungsten, and  $La_2O_3$ -doped W.

## 2. Experimental

Experiments were performed with a high flux ion beam test device (HiFIT) [8,9]. With this device, several ion species such as molecular hydrogen ions and small amount of impurity ions are simultaneously impinged onto samples due to no mass selection. Hydrogen ion species are combination of  $H_3^+$ ,  $H_2^+$ , and  $H^+$ . Hydrogen atom species ratios irradiated to samples were 70–80% for 333 eV H and 10–15% for 500 eV H and 1 keV H (acceleration voltage was 1 kV). Carbon impurity ions of about 0.8% were deliberately introduced in hydrogen ion beams to enhance blister formation. The other impurity concentrations were less than about 0.1%. The enhancement of blister formation with carbon impurities in ion beams was observed for all tungsten materials used in this study [10]. Carbon impurities were included in ion beams as hydrocarbon molecular ions such as  $CH_x^+$  and  $C_2H_y^+$ . Therefore, the energies of carbon atoms were slightly less than 1 keV and 500 eV. The sample temperature was set at 653 K for all experiments.

Tungsten samples used for this study are pure W with the purity of more than 99.99 wt%, K-doped W with 28 wppm of K, and  $La_2O_3$  doped W with about 0.96 wt%  $La_2O_3$ . A sample size was 10 mm × 20 mm with the thickness of 1 mm. Ion beam irradiation area was 3 mm $\phi$ , determined by a circular aperture placed just in front of the samples. The sample surfaces were mirror polished mechanically to the roughness of less than 0.1  $\mu$ m. The W samples were fabricated by powder metallurgy supplied by A.L.M.T. Co. A hot rolling process with 900–1600 °C was done to make 1 mm thickness plates. Then all samples were annealed at 900 °C for 0.5 h to relieve internal stresses. For recrystallization, annealing of pure W at 1300 °C for 1 h was enough, while for K-doped W and  $La_2O_3$ -doped W, 1500 °C for 1 h was needed. By this recrystallization process, average grain sizes became 21  $\mu$ m for pure W, 29  $\mu$ m for K-doped W, and 39  $\mu$ m for  $La_2O_3$ -doped W. In this

paper, the samples without heat treatment for recrystallization are called ‘stress relieved’ or ‘SR’ and the recrystallized samples are called ‘recrystallized’ or ‘RE’. For K-doped W, K atoms were mainly distributed at grain boundaries and some of them in grains. For  $La_2O_3$ -doped W, small particulates of  $La_2O_3$  were distributed linearly parallel to the irradiation surface with lengths of a few  $\mu$ m to several tens of  $\mu$ m [11]. These particulates exist not only at grain boundaries but also in grains.

## 3. Experimental results and discussions

Fig. 1 shows surface morphologies of pure W samples after ion beam irradiation (stress relieved (a) and recrystallized (b)) and microstructures (stress relieved (c) and recrystallized (d)). They were irradiated by 1 keV  $H_3^+$  (main ion component) to the fluence of about  $1 \times 10^{25}$  H/m $^2$ . For SR pure W (Fig. 1(a)), the shapes of most blisters were almost spherical-like with sizes ranged from about 5  $\mu$ m to 210  $\mu$ m. The number density was 450 blisters/mm $^2$ . Blister size distributions of pure W samples are shown in Fig. 2. The number of blisters with the sizes around 10  $\mu$ m was the largest. Some of the large blisters showed cracks on the surface but no exfoliation was found. For RE pure W (Fig. 1(b)), the shapes of blisters were different from those of SR pure W. Although some of the blisters had spherical-like shapes similar to SR pure W, most of the blisters had more complicated plateau-like shapes. Blister sizes ranged from about 5  $\mu$ m to 100  $\mu$ m. There existed only a few small blisters with the sizes less than 10  $\mu$ m. The number density was 140 blisters/mm $^2$ , much less than that of SR pure W. A lot of blisters had cracks on their surfaces and some of them fell off in flakes.

Blister shapes for pure W had a close relation with microstructure. The microstructure of SR pure W was

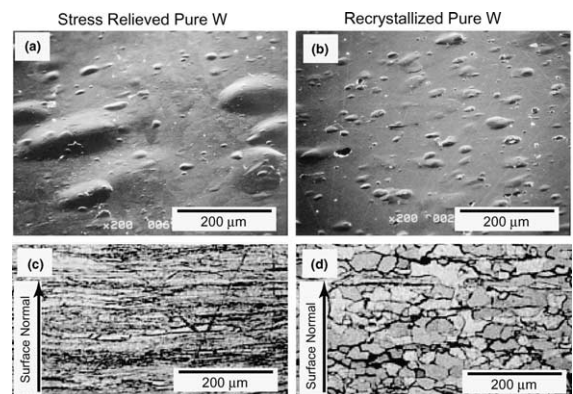


Fig. 1. Surface morphologies (a, b) and microstructures (c, d) for stress relieved and recrystallized pure W after 1 keV  $H_3^+$  ion beam irradiation at 653 K to the fluence of  $1 \times 10^{25}$  H/m $^2$ .

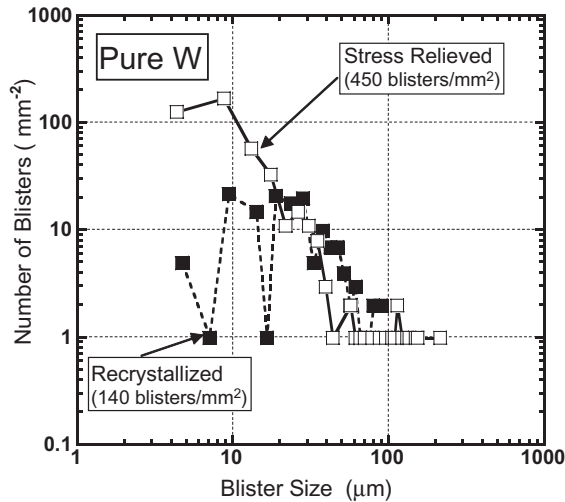


Fig. 2. Blister size distributions for stress relieved and recrystallized pure W.

layered with high elongation grains arranged parallel to the surface, see Fig. 1(c). More detailed measurements by FIB (focused ion beam) showed that the width of the grains (perpendicular to the surface) was a few  $\mu\text{m}$ . Hydrogen bubbles tend to be formed and grow in grain boundaries and decrease adhesion between grains. When blistering takes place, internal cracks are generated mainly in grain boundaries. These cracks grow along grain boundaries, almost parallel to the surface for SR pure W. Eventually, internal pressure of hydrogen in internal cracks or internal compressive stress induced by hydrogen solution in grains drove plastic surface deformation. The compressive internal stress could be caused by H-atoms or H-bubbles in the interstitial sites. In this process, blister shapes became almost spherical, and thickness of the blister lid and the blister size had a close relation: the thickness of the lids was roughly one order of magnitude smaller than the blister size.

On the other hand, RE pure W had low elongation grains (average aspect ratio of about 1.6) with an average grain size of  $21\mu\text{m}$ , much larger than the thickness of the layers in SR pure W, see Fig. 1(d). From Fig. 2, the blister sizes of RE pure W are distributed mainly between  $10\mu\text{m}$  and  $50\mu\text{m}$ , which are closely correlated with the grain size. In the process of blister formation for RE pure W, internal cracks were generated by accumulation of hydrogen bubbles in the grain boundaries. These cracks, however, did not propagate much and the length of the cracks was almost limited to the grain size. In this case, the thickness of the blister lid was too thick compared with the blister size to form spherical-like blisters. Then the blister lid moved up by internal stress in the grain without significant plastic deformation. This process resembles formation of a reverse fault in the earth's crust.

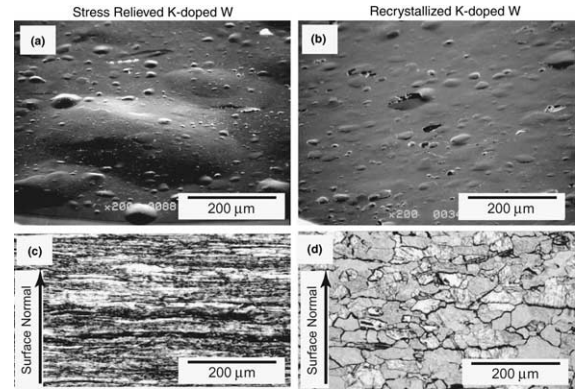


Fig. 3. Surface morphologies (a,b) and microstructures (c,d) for stress relieved and recrystallized K-doped W after  $1\text{keV H}^+$  ion beam irradiation at  $653\text{K}$  to the fluence of  $1 \times 10^{25}\text{H/m}^2$ .

Surface morphologies and microstructures of K-doped W are shown in Fig. 3. In general, blister shapes and microstructures for SR and RE K-doped W are similar to those of pure W. The most notable difference between pure W and K-doped W was the number of blisters. For SR K-doped W, the blister size ranged from about  $5\mu\text{m}$  to  $250\mu\text{m}$  and the number density was  $2100\text{ blisters/mm}^2$ , which is about five times more than that of SR pure W. From the blister size distributions of K-doped W in Fig. 4, blisters with sizes between  $5\mu\text{m}$  and  $20\mu\text{m}$  contributed to this difference. For RE K-doped W, the blister size ranged from  $2\mu\text{m}$  to  $100\mu\text{m}$  and the number density was  $2260\text{ blisters/mm}^2$ , which was an order of magnitude larger than that of RE pure W. The small blisters with the sizes less than  $20\mu\text{m}$  also contributed this difference, see Fig. 4.

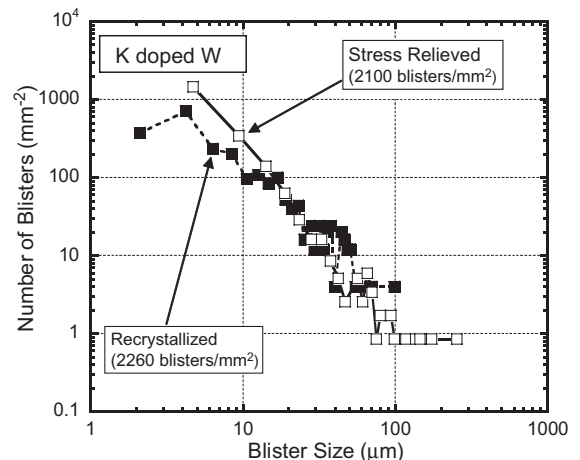


Fig. 4. Blister size distributions for stress relieved and recrystallized K-doped W.

For both SR and RE K-doped W, the number of small blisters with sizes less than 20 μm was much greater than that of pure W. Since the microstructure of K-doped W and pure W did not differ much, the difference in the number density of small blisters could be attributed to the effect of the K dopant. In general, K dopants were distributed mainly in grain boundaries (some of them were distributed in grains). K dopants in grain boundaries could be traps for hydrogen to enhance delamination of grains. In addition, K dopants in grains would increase hydrogen solution in the grains, leading to enhancement of internal stress, especially in the top thin surface layer. This increase in high internal stress as well as enhancement of delamination could promote formation of small blisters.

Surface morphologies and microstructures of La<sub>2</sub>O<sub>3</sub>-doped W were shown in Fig. 5. For SR La<sub>2</sub>O<sub>3</sub>-doped W, the dominant blisters were plateau-like ones similar to recrystallized W, though some spherical-like blisters and large blisters with the sizes more than 100 μm, characteristic of stress relieved W, were observed, see Fig. 5(a). This could be attributed to the microstructure of SR La<sub>2</sub>O<sub>3</sub>-doped W, in which grain growth already started to form large grains with low elongation, and the layered structures were somewhat disordered, see Fig. 5(c). For RE La<sub>2</sub>O<sub>3</sub>-doped W, quite a lot of blisters with large cracks and exfoliations were observed. In this case, some cracks and exfoliations were already produced in the process of mechanical polishing before ion irradiation. Therefore, the exfoliations on RE La<sub>2</sub>O<sub>3</sub>-doped W in Fig. 5(b) were produced either by mechanical polishing or hydrogen ion irradiation. This indicated that RE La<sub>2</sub>O<sub>3</sub>-doped W was a very brittle material even without hydrogen ion beam irradiation. Fig. 6 shows the blister size distribution for La<sub>2</sub>O<sub>3</sub>-doped W, in which the size distribution of exfoliations

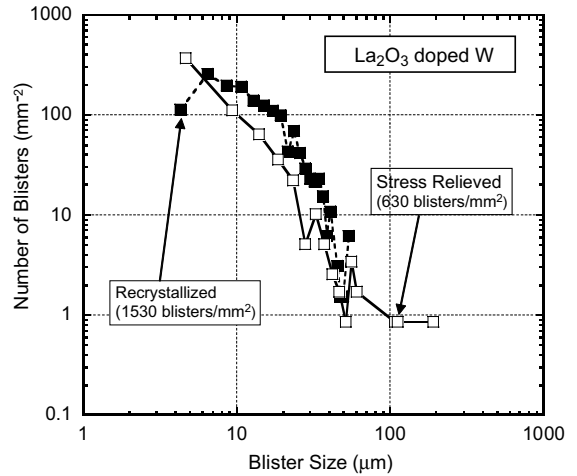


Fig. 6. Blister size distributions for stress relieved and recrystallized La<sub>2</sub>O<sub>3</sub>-doped W.

produced only by mechanical polishing was subtracted. For RE La<sub>2</sub>O<sub>3</sub>-doped W, the number of small blisters with sizes less than about 20 μm was very large, similar to RE K-doped W.

The fluence dependence of the number of blisters showed different features for each tungsten, see Fig. 7. For doped W, the number of blisters did not change significantly with fluences from about 3 × 10<sup>24</sup> H/m<sup>2</sup> to 1 × 10<sup>25</sup> H/m<sup>2</sup>, while for pure W the number was increased for both SR and RE. It is noted that for RE pure W, no blisters were observed at 3 × 10<sup>24</sup> H/m<sup>2</sup> but they appeared at 1 × 10<sup>25</sup> H/m<sup>2</sup>. For long burn fusion reactors (a year or more), ion fluence to first walls would be as high as 10<sup>28</sup> D/m<sup>2</sup>. Therefore, higher fluence data or

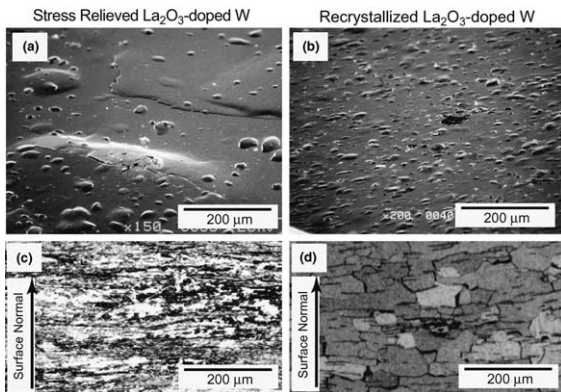


Fig. 5. Surface morphologies (a, b) and microstructures (c, d) of stress relieved and recrystallized La<sub>2</sub>O<sub>3</sub>-doped W after 1keV H<sub>3</sub><sup>+</sup> ion beam irradiation at 653 K to the fluence of 1 × 10<sup>25</sup> H/m<sup>2</sup>.

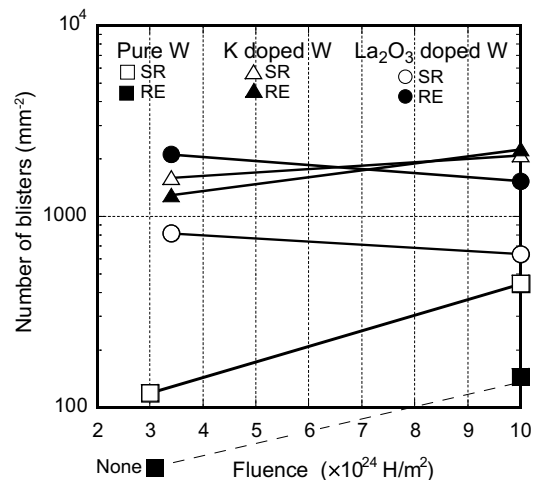


Fig. 7. Fluence dependence of blister number density for pure W, K-doped W, and La<sub>2</sub>O<sub>3</sub>-doped W. SR and RE denote ‘stress relieved’ and ‘recrystallized’.

reliable extrapolation models are necessary to apply these data under fusion relevant fluence conditions.

For pure W, the recrystallization process reduced the number of blisters, which indicated that hydrogen trapping sites such as grain boundaries and dislocations decreased. On the other hand, for the two doped W materials, the number of blisters did not change much for K-doped W by recrystallization or even increased for La<sub>2</sub>O<sub>3</sub>-doped W, indicating that these dopants could be dominant traps for hydrogen or play a dominant role in controlling hydrogen diffusion. In addition, especially for recrystallized La<sub>2</sub>O<sub>3</sub>-doped W these dopants could reduce adhesion between grains.

#### 4. Conclusion

Blister characteristics and cracking behavior of tungsten under hydrogen ion irradiation strongly depend on microstructures and dopant materials. For W materials with layered microstructure, blister shapes were mostly spherical-like, while for W with recrystallized (or disordered) microstructures, they were plateau-like. Addition of K or La<sub>2</sub>O<sub>3</sub> dopants increased the number of blisters and exfoliations. From above mentioned viewpoints, pure W showed better performance under hydrogen

ion irradiation environments than K-doped or La<sub>2</sub>O<sub>3</sub>-doped W under present experimental conditions.

#### References

- [1] Y. Ueda, K. Tobita, Y. Katoh, J. Nucl. Mater. 313–316 (2003) 32.
- [2] A. Haasz, M. Poon, J. Davis, J. Nucl. Mater. 266–269 (1999) 520.
- [3] T. Venhaus, T. Abeln, R. Doerner, R. Causey, J. Nucl. Mater. 290–293 (2001) 505.
- [4] W. Wang, J. Roth, S. Lindig, C. Wu, J. Nucl. Mater. 299 (2001) 124.
- [5] T. Shimada, H. Kikuchi, Y. Ueda, A. Sagara, M. Nishikawa, J. Nucl. Mater. 313–316 (2003) 204.
- [6] T. Shimada, Y. Ueda, M. Nishikawa, Fusion Eng. Des. 66–68 (2003) 247.
- [7] Y. Ueda, T. Shimada, M. Nishikawa, Nucl. Fusion 44 (2004) 62.
- [8] T. Shimada, Y. Ueda, A. Sagara, M. Nishikawa, Rev. Sci. Instrum. 73 (2002) 1741.
- [9] Y. Ueda, H. Kikuchi, T. Shimada, A. Sagara, B. Kyoh, M. Nishikawa, Fusion Eng. Des. 61&62 (2002) 255.
- [10] T. Funabiki, T. Shimada, Y. Ueda, M. Nishikawa, J. Nucl. Mater. (2004).
- [11] Private communication from A.L.M.T. Co.